Magnetic imaging by Fourier transform holography using linearly polarized x-rays

Maurizio Sacchi, H. Popescu, N. Jaouen, M. Tortarolo, F. Fortuna, R. Delaunay, C. Spezzani

▶ **To cite this version:**

Maurizio Sacchi, H. Popescu, N. Jaouen, M. Tortarolo, F. Fortuna, et al.. Magnetic imaging by Fourier transform holography using linearly polarized x-rays. Optics Express, 2012, 20, pp.9769-9776. 10.1364/OE.20.009769 . in2p3-00713713

HAL Id: in2p3-00713713
https://hal.in2p3.fr/in2p3-00713713

Submitted on 8 Jun 2022

HAL is a multi-disciplinary open access archive for the deposit and dissemination of scientific research documents, whether they are published or not. The documents may come from teaching and research institutions in France or abroad, or from public or private research centers.

L'archive ouverte pluridisciplinaire **HAL**, est destinée au dépôt et à la diffusion de documents scientifiques de niveau recherche, publiés ou non, émanant des établissements d'enseignement et de recherche français ou étrangers, des laboratoires publics ou privés.

Distributed under a Creative Commons Attribution 4.0 International License

Magnetic imaging by Fourier transform holography using linearly polarized x-rays

Maurizio Sacchi,[1,2,*] Horia Popescu,[2] Nicolas Jaouen,[2] Marina Tortarolo,[2] Franck Fortuna,[3] Renaud Delaunay,[4] and Carlo Spezzani[5]

[1] *Institut des NanoSciences de Paris, UPMC Paris 06, CNRS UMR 7588, 4 Pl. Jussieu, 75015 Paris, France*
[2] *Synchrotron SOLEIL, L'Orme des Merisiers, Saint-Aubin, B.P. 48, 91192 Gif-sur-Yvette, France*
[3] *Centre de Spectrométrie Nucléaire et Spectrométrie de Masse, Université Paris-Sud, Bât. 104, 91405 Orsay, France*
[4] *Laboratoire de Chimie Physique - Matière et Rayonnement, UPMC Paris 06, CNRS UMR 7614, 11 rue P. et M. Curie, 75005 Paris, France*
[5] *ELETTRA, Sincrotrone Trieste, Area Science Park, S.S.14, Km 163.5, 34012 Trieste, Italy*
[*] *maurizio.sacchi@synchrotron-soleil.fr*

Abstract: We present a method for imaging magnetic domains via x-ray Fourier transform holography at linearly polarized sources. Our approach is based on the separation of holographic mask and sample and on the Faraday rotation induced on the reference wave. We compare images of perpendicular magnetic domains obtained with either linearly or circularly polarized x-rays and discuss the relevance of this method to future experiments at free-electron laser and high-harmonic-generation sources.

© 2012 Optical Society of America

OCIS codes: (340.7440) X-ray imaging; (300.6560) Spectroscopy, x-ray; (160.3820) Magneto-optical materials; (230.5440) Polarization-selective devices.

References and links

1. S. Eisebitt, J. Lüning, W. F. Schlotter, M. Lörgen, O. Hellwig, W. Eberhardt, and J. Stöhr, "Lensless imaging of magnetic nanostructures by X-ray spectro-holography," Nature **432**(7019), 885–888 (2004).
2. S. Roy, D. Parks, K. A. Seu, R. Su, J. J. Turner, W. Chao, E. H. Anderson, S. Cabrini, and S. D. Kevan, "Lensless x-ray imaging in reflection geometry," Nat. Photonics **5**, 243–245 (2011).
3. C. Tieg, R. Frömter, D. Stickler, S. Hankemeier, A. Kobs, S. Streit-Nierobisch, C. Gutt, G. Grübel, and H. P. Oepen, "Imaging the in-plane magnetization in a Co microstructure by Fourier transform holography," Opt. Express **18**(26), 27251–27256 (2010).
4. see, e.g., LCLS proposals L134, L148, L197, L396, L409 of the SXR beamline (*http://www-ssrl.slac.stanford.edu/lcls/users/schedules.html*).
5. B. Vodungbo, A. Barszczak Sardinha, J. Gautier, G. Lambert, C. Valentin, M. Lozano, G. Iaquaniello, F. Delmotte, S. Sebban, J. Lüning, and P. Zeitoun, "Polarization control of high order harmonics in the EUV photon energy range," Opt. Express **19**(5), 4346–4356 (2011).
6. B. Pfau, C. M. Günther, R. Könnecke, E. Guehrs, O. Hellwig, W. F. Schlotter, and S. Eisebitt, "Magnetic imaging at linearly polarized x-ray sources," Opt. Express **18**(13), 13608–13615 (2010).
7. W. F. Schlotter, J. J. Turner, M. Rowen, P. Heimann, M. Holmes, O. Krupin, M. Messerschmidt, S. Moeller, J. Krzywinski, R. Soufli, M. Fernndez-Perea, N. Kelez, S. Lee, R. Coffee, G. Hays, M. Beye, N. Gerken, F. Sorgenfrei, S. Hau-Riege, L. Juha, J. Chalupsky, V. Hajkova, A. P. Mancuso, A. Singer, O. Yefanov, I. A. Vartanyants, G. Cadenazzi, B. Abbey, K. A. Nugent, H. Sinn, J. Lning, S. Schaffert, S. Eisebitt, W.-S. Lee, A. Scherz, A. R. Nilsson, and W. Wurth, "The soft x-ray instrument for materials studies at the linac coherent light source x-ray free-electron laser," Rev. Sci. Instrum. (to be published).
8. D. Stickler, R. Frömter, H. Stillrich, C. Menk, C. Tieg, S. Streit-Nierobisch, M. Sprung, C. Gutt, L.-M. Stadler, O. Leupold, G. Grübel, and H. P. Oepen, "Soft x-ray holographic microscopy," Appl. Phys. Lett. **96**, 042501 (2010).
9. P. Carra, B. T. Thole, M. Altarelli, and X. Wang, "X-ray circular dichroism and local magnetic fields," Phys. Rev. Lett. **70**(5), 694–697 (1993).
10. J. J. Turner, X. Huang, O. Krupin, K. A. Seu, D. Parks, S. Kevan, E. Lima, K. Kisslinger, I. McNulty, R. Gambino, S. Mangin, S. Roy, and P. Fischer, "X-ray diffraction microscopy of magnetic structures," Phys. Rev. Lett. **107**(3), 033904 (2011).
11. J. B. Kortright and S.-K. Kim, "Resonant magneto-optical properties of Fe near its 2*p* levels: measurement and applications," Phys. Rev. B **62**, 12216–12228 (2000).
12. E. Guehrs, C. M. Günther, B. Pfau, T. Rander, S. Schaffert, W. F. Schlotter, and S. Eisebitt, "Wavefield back-propagation in high-resolution X-ray holography with a movable field of view," Opt. Express **18**(18), 18922–18931 (2010).

#163638 - $15.00 USD Received 23 Feb 2012; revised 6 Apr 2012; accepted 7 Apr 2012; published 13 Apr 2012
(C) 2012 OSA

13. P. N. Argyres, "The theory of Faraday and Kerr effects in ferromagnetics," Phys. Rev. **97**, 334–345 (1955).
14. C. Spezzani, "Diffusion résonante des rayons X polarisés et couplage magnétique dans les multicouches Co/Cu," Ph.D. Thesis, University of Paris XI, OCLC n.491574486 (2003).
15. A. Scherz, W. F. Schlotter, K. Chen, R. Rick, J. Stöhr, J. Lüning, I. McNulty, C. Günther, F. Radu, W. Eberhardt, O. Hellwig, and S. Eisebitt, "Phase imaging of magnetic nanostructures using resonant soft x-ray holography," Phys. Rev. B **76**, 214410 (2007).
16. M. Sacchi, N. Jaouen, H. Popescu, R. Gaudemer, F. Polack, B. Lagarde, G. Cauchon, A. Delmotte, J.-M. Dubuisson, J.-M. Tonnerre, G.-S. Chiuzbaian, and C. F. Hague, "The SEXTANTS beamline at SOLEIL: a new facility for elastic, inelastic and coherent scattering of soft x-rays," in *Proceedings of the 11th International Conference on Synchrotron Radiation Instrumentation (SRI 2012)*, J. Phys. Conf. Ser. (to be published).
17. M. Sacchi, H. Popescu, R. Gaudemer, N. Jaouen, A. Avila, R. Delaunay, U. Maier, and C. Spezzani, "IRMA-2 at SOLEIL: a set-up for magnetic and coherent scattering of polarized soft x-rays," in *Proceedings of the 11th International Conference on Synchrotron Radiation Instrumentation (SRI 2012)*, J. Phys. Conf. Ser. (to be published).

1. Introduction

Soft x-ray magnetic imaging by Fourier transform holography (FTH) has found many new applications in recent years [1–3]. Particularly attractive perspectives are the development of FTH imaging at high-harmonic-generation (HHG) laser-based laboratory sources and single-shot femtosecond time-resolved imaging using linac-based x-ray free-electron lasers [4]. Among many exceptional characteristics of these sources there is up to now one limitation, i.e. the fixed linear polarization state of the x-rays. This affects negatively FTH imaging of magnetic domains, which is performed using circularly polarized light. At very low photon energy, e.g., at the 3p resonances of 3d transition metals (TM), reflection-based polarizers can be employed [5]. At the TM 2p and rare-earth (RE) 3d resonances, elliptical polarization is currently obtained by inserting a Faraday polarizer containing the element of interest [6,7].

Here we show that perpendicular magnetic domains can be imaged by Fourier transform holography using linearly polarized x-rays directly. Our approach is based on separating the sample from the holographic mask [8] and on making the reference beam go through the magnetized sample. In this way, we effectively integrate a Faraday polarizer for the reference wave into the sample-mask ensemble, with potential improvement of the experimental conditions with respect to the use of a separate filter.

Imaging by FTH relies on the interference between coherent beams scattered by the object to be imaged and by one or more reference holes, whose size contributes to define the overall spatial resolution [1]. In the most common approach, one deposits the sample on one side of a highly transparent membrane (e.g., Si_3N_4), and a thick x-ray absorbing layer (e.g., 1μm Au) on the opposite side. The object is then defined by removing the absorbing layer over the area to be imaged, while each aperture defining a reference wave is obtained by opening a through-hole in the stack; usually, these operations are performed by focused ion beam (FIB) milling. At the price of a fixed field of view (FOV), the main interest of the integrated mask-sample approach is the stability inherent to the system, which makes even long measurements virtually insensitive to vibrations or drifts.

When the sample is illuminated by a coherent wave-front, the spatial distribution of the optical constants within the object area generates a unique angular distribution of the scattered wave and this information is coded in phase and amplitude at the detector level, via the interference with the reference wave. The Fourier transform (FT) of the two-dimensional (2D) map of scattered intensities corresponds to the autocorrelation function of the entire sample (object and reference). By an appropriate sample design, the cross-correlation between object and reference can be well separated from the self-correlation of each one of them, providing an image of the object with a resolution limited primarily by the diameter of the reference through-hole [1–3].

For imaging magnetic domains, one tunes the photon energy at a core absorption resonance and relies on x-ray magnetic circular dichroism (XMCD) [9]: since the absorption coefficient (hence the optical index) depends on the sign of the magnetization, each given magnetic domain distribution within the object produces a specific diagram in coherent

#163638 - $15.00 USD Received 23 Feb 2012; revised 6 Apr 2012; accepted 7 Apr 2012; published 13 Apr 2012
(C) 2012 OSA

scattering. In the 2D-FT of the scattering signal, the object-reference cross-correlation will image the magnetic domain structure as dark/bright areas, the intensity being related to the local projection of the magnetization along the propagation direction of the incoming x-rays.

It is well known that resonant scattering of linearly polarized x-rays is sensitive to the magnetic properties of the sample and, in particular, it was shown recently that magnetic structures can be investigated by coherent scattering in transmission mode [10]. This is because transmission through a magnetic material induces a rotation of the linear polarization vector with opposite handedness according to the magnetization direction (x-ray Faraday rotation [11],). The interference between waves scattered at domains with opposite magnetization generates magnetic speckle. In a holographic experiment, though, the reference wave retains the original polarization direction and cannot interfere with the orthogonal magnetization-sensitive component of the wave scattered by the sample. As a consequence, the 2D-FT does not provide an image of the magnetic structure of the sample.

In our experiment, we take advantage of an alternative approach to sample/mask preparation, originally proposed by Stickler *et al.* [8], where the sample (deposited on one transparent membrane) and the mask (with the object and reference apertures carved in an opaque Au film) are physically separated and can be aligned individually with respect to the x-ray beam. In this way, one can displace the FOV and image any selected area of the sample. Although requiring a more complex alignment set-up, this approach simplifies sample preparation and FIB machining. Since sample and mask do not pertain to the same plane anymore, either they are brought close enough to be within the depth of focus of the technique or analytical corrections must be applied [12].

What is of interest to our work is that, in this set-up, the linearly polarized reference wave traverses the magnetic sample, undergoing Faraday rotation [13]. Both object and reference scattered waves will have rotated polarization components and will interfere at the detector level; therefore, a magnetization-related contrast in the FT intensity is expected.

The optical index n of a magnetic material differs for circularly polarized photons of opposite helicity ($\pm$) propagating along the magnetization axis:

$$n^{\pm} = 1 - \delta^{\pm} - i\beta^{\pm} = n^{\circ} \pm \Delta\delta/2 \pm i\Delta\beta/2,$$

where $n^{\circ} = 1 - \delta^{\circ} - i\beta^{\circ}$ is the magnetization averaged index and $\Delta\delta$ and $\Delta\beta$ represent the real and imaginary parts of $(n^{+} - n^{-})$. Linearly polarized radiation can be described as the coherent superposition of right and left circularly polarized components. A finite $\Delta\delta$ induces a phase difference between the two components [13], resulting in a rotation φ of the polarization axis upon transmission through a magnetic material; the Faraday rotation angle φ is linearly proportional to $\Delta\delta$ and to the traversed thickness t, i.e., $\varphi(\lambda) = \pi t\Delta\delta(\lambda)/\lambda$. A finite $\Delta\beta$ implies a different absorption for the two circular components [13], resulting in an induced ellipticity of the outgoing wave; defining χ as the ratio between the minor to major axis of the outgoing polarization ellipse, one has $\chi(\lambda) = \tanh[\pi t\Delta\beta(\lambda)]$, leading to a circular polarization rate $P(\lambda) = 2\chi(\lambda)/[1 + \chi^2(\lambda)]$. The magnetization averaged (δ°, β°) and magnetization dependent ($\Delta\delta$, $\Delta\beta$) terms of the optical constants of Co at the 2p resonance are given in Fig. 1(a) and Fig. 1(b), respectively [14]. Figure 1(c) shows the values of φ, χ and of the magnetization averaged transmission across the L_3 resonance for 80nm of Co (sample of Figs. 2-5). A maximum Faraday rotation of 18.8° (i.e., 0.235°/nm) is attained at 777 eV, with a transmission larger than 15%. Maximum ellipticity (corresponding to a polarization rate of 85%) is obtained at the L_3 absorption maximum (778 eV), with a transmission lower than 2%.

#163638 - $15.00 USD Received 23 Feb 2012; revised 6 Apr 2012; accepted 7 Apr 2012; published 13 Apr 2012
(C) 2012 OSA

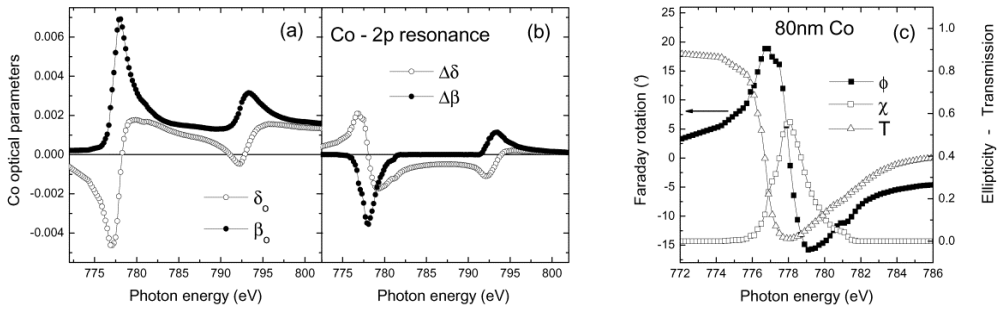

Fig. 1. (a): magnetization averaged optical constants of metallic Co [14]. (b): magnetization dependent part of the optical constants for magnetically saturated Co [14]. (c): transmission (T), Faraday rotation (φ) and ellipticity (χ) for an 80nm thick Co film.

Since φ and Δβ functions peak at two different energies, one expects that imaging based on absorption contrast (XMCD) and dispersive contrast (Faraday effect) will be optimized at slightly different energies [15].

2. Experimental details

$(Co_x/Pd_y)_n$ multilayers with x = 0.4nm, y = 0.8nm and n = 200 were prepared by magnetron sputtering on a 100nm thick Si_3N_4 membrane (250 × 250μm^2 window on a 200μm thick Si frame). Two extra layers of Pd were used as buffer and protective layers. The samples were characterized by MOKE and MFM, displaying strong perpendicular anisotropy and a meander domain structure with a period of approximately 450nm. In-plane demagnetization cycles were applied prior to scattering experiments, favoring the parallel alignment of stripe domains. Several masks were prepared by FIB, starting from $(Au_{50nm}/Cr_{5nm})_{20}$ multilayered films sputter-deposited on Si_3N_4 membranes. The diameter of the circular object aperture ranged from 0.7 to 3 μm. Reference apertures (3 per mask, with nominal diameters from 50nm to 150nm) were placed at a distance of 2.5 object-diameters from the center of the object aperture. This guarantees that no overlap occurs in the FT between the object self-correlation and the object-reference cross-correlation. Object and reference apertures of the mask were through holes, making the FIB machining much simpler with respect to the integrated mask/sample design. Both (Co/Pd) and (Au/Cr) layers were deposited on the side of the Si_3N_4 membrane where the Si frame is located. Therefore, by approaching their Si_3N_4 uncovered sides, we could bring them in close contact without risking any damage to the films.

Resonant coherent scattering experiments were carried out at the SEXTANTS beamline of the SOLEIL synchrotron [16]. The beamline features two helical undulators which provide full polarization control over the 50-1700eV energy range. Working at the fundamental emission line of the 44mm period undulator, estimated polarization rates at the Co 2p resonances exceed 98% for both linear horizontal and left/right circular modes. The central emission from the undulator (40 × 40μrad^2) was selected using diaphragms; the transverse coherence length of the beam at the sample position was monitored using a test-mask with an array of apertures, obtaining values in excess of 20μm in both horizontal and vertical directions. The energy resolving power of the monochromator was 8000, setting the longitudinal coherence length to approximately 12μm. The experiment took place at the intermediate focal point of the elastic scattering branch, using the IRMA-2 scattering chamber [17]. Samples and masks were mounted on two independent positioning stages, both bolted onto the same optical bench inside the vacuum chamber, in order to minimize the relative sample–mask vibrations. Tending to the same end, measurements were taken with the sample and the mask in contact. By defining Y as the horizontal beam propagation direction, masks could be aligned along (X,Z) and samples along (X,Y,Z), with 50nm encoded positioning of

#163638 - $15.00 USD Received 23 Feb 2012; revised 6 Apr 2012; accepted 7 Apr 2012; published 13 Apr 2012
(C) 2012 OSA

the samples. Measurements were performed at the Co $2p_{3/2}$ resonance, using either circular (left/right) or linear (horizontal) polarization. 2D scattering diagrams were collected using a back-illuminated CCD camera placed 450mm behind the sample, covering a range of 226μm^{-1} in both q_x and q_z (projections of the exchanged momentum on the sample surface). Single-frame exposure time varied from 0.1s to 3s depending on sample (amount of Co), mask (object hole size) and photon energy (on/off resonance). Good quality images required the acquisition of about 100 frames. In order to prevent visible stray light to reach the camera, a light-tight filter (100nm Al coated parylene) was mounted in front of it. A beamstop (300μm diameter sphere on a 10μm thick wire) was placed just in front of the CCD filter. Its position could be adjusted via two piezoelectric motors, in order to block the intense transmitted beam.

3. Results

Figure 2(a) shows a scattering diagram collected at 777 eV using linearly polarized radiation, where intense magnetic speckle is clearly visible. A line is drawn through the speckle region and its profile is shown in Fig. 2(b), as a function of the photon energy. The magnetic-related signal peaks at 777 eV, i.e. ~1eV below the absorption maximum.

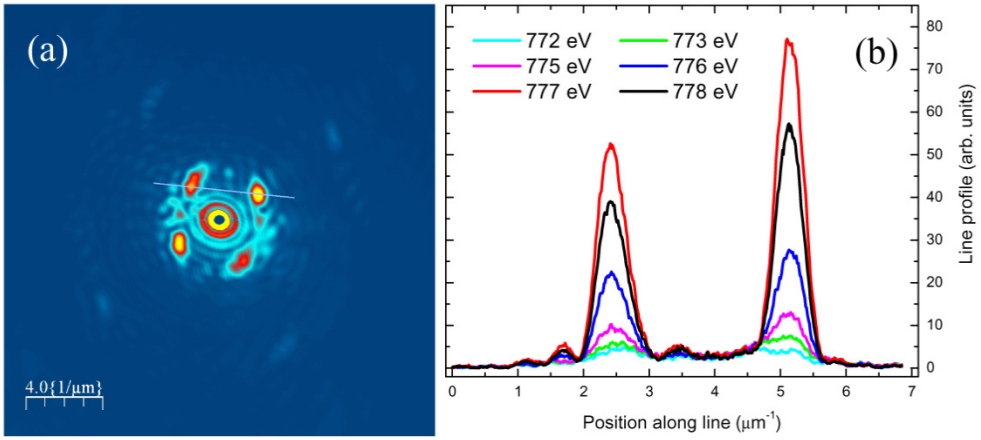

Fig. 2. (a): Scattering diagram collected using 777eV linearly polarized photons. (b): intensity profile along the line drawn through the magnetic speckle, as a function of photon energy.

The sign of the magnetization in the sample area traversed by the reference wave defines the vertical component of its polarization, hence the magnetic contrast in the FTH image. Therefore, traversing a domain boundary may affect the image negatively. It should be noted, though, that reference holes must be smaller than the desired spatial resolution, hence smaller than the expected domain size. Moreover, independent displacement of sample and mask with a stepsize (5nm, in our set-up) that is much finer than the domain width can be used to control the area traversed by the reference wave in order to optimize the magnetic contrast.

Figure 3(a) shows part of the scattering diagram for the Co/Pd multilayer illuminated by 777eV linearly polarized photons through a FTH mask featuring a 1.7μm object aperture. Magnetic speckle and interference with reference waves are clearly visible. The part of the FT containing the sample (object and references) autocorrelation is shown in Fig. 3(b). Only two independent reference-object cross-correlation images are visible (plus their complex conjugates), the third one being too weak to show.

#163638 - $15.00 USD Received 23 Feb 2012; revised 6 Apr 2012; accepted 7 Apr 2012; published 13 Apr 2012
(C) 2012 OSA

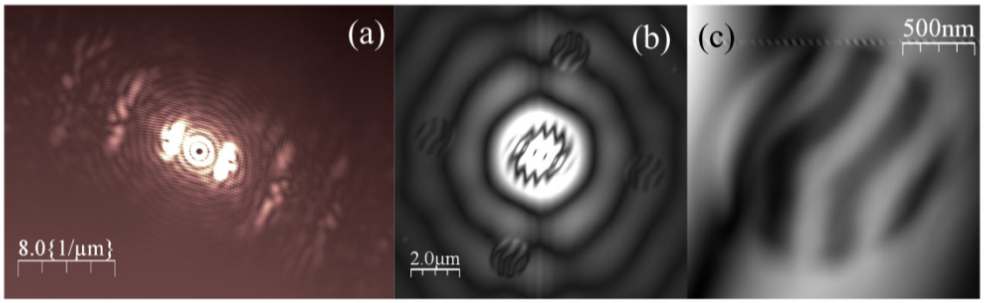

Fig. 3. (a) Scattering diagram collected using 777eV linearly polarized photons. (b) Selected area of the FT showing the sample autocorrelation, with two independent reference-object cross-correlation images. (c) Zoom on the right side cross-correlation image.

The FT of Fig. 3(b) is dominated by annular modulations, coming from the presence of the beam-stop in the scattering diagram of Fig. 3(a). Since our primary interest is to compare images of perpendicular magnetic domains taken with either linearly or circularly polarized photons, we will show only FTH images obtained by a single acquisition (one photon energy, one polarization state), without any data reduction or correction beyond a simple 2D-FT. Therefore, we do not correct for the presence of the beam-stop, although it introduces strong modulations in the FT image, and we do not apply any back-propagation algorithm to correct for an eventual separation between mask and sample planes [12]. Nonetheless, the zoom on a single object-reference cross-correlation image of Fig. 3(c) shows a very clear contrast related to the formation of ordered stripes of perpendicular magnetic domains. The magnetic period of ~500nm matches perfectly the results of MFM microscopy.

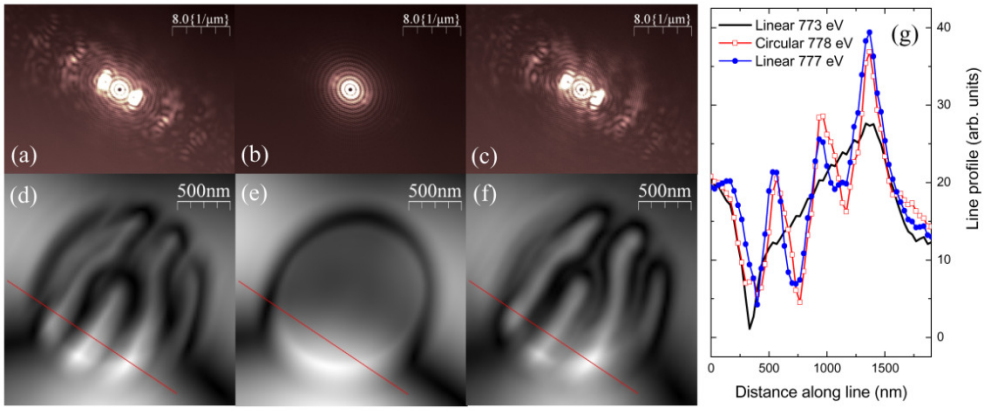

Fig. 4. Scattering diagrams collected using linearly polarized x-rays at 777eV (a) and 773eV (b), and circularly polarized x-rays at 778eV (c). Selected FT areas containing an object-reference cross-correlation image are shown below each diagram [(d), (e) and (f), respectively]. The intensity profiles along the lines drawn through the FT images are compared in (g).

Figure 4 compares results obtained on a different area of the same sample, using linear polarization at the $\Delta\delta$ maximum [777 eV, Figs. 4(a), 4(d)] and off-resonance [773 eV, Fig. 4(b), 4(e)], and circular polarization at the $\Delta\beta$ maximum [778 eV, Figs. 4(c), 4(f)]. Selected areas of the scattering diagrams and of the corresponding 2D-FT are shown Figs. 4(a)-4(c) and Fig. 4(d)-4(f), respectively. The three images were acquired with equivalent statistics (integration times of 20s, 140s and 400s, respectively) and normalized to the intensity close to the center (around the beam-stop). In Fig. 4(g), line-scans across the FT images show that the modulations related to magnetic order are of comparable magnitude for resonant scattering

#163638 - $15.00 USD Received 23 Feb 2012; revised 6 Apr 2012; accepted 7 Apr 2012; published 13 Apr 2012
(C) 2012 OSA

measurements performed with either linear or circular polarization. These modulations appear as oscillations around the straight line measured off-resonance.

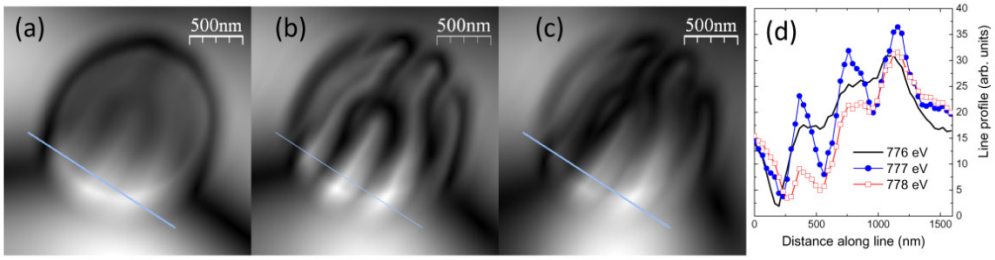

Fig. 5. FTH images obtained using linearly polarized x-rays of 776eV (a), 777eV (b) and 778eV (c) photon energy. The intensity profiles along the lines drawn through the images are compared in (d).

Figure 5 illustrates the energy dependence of FTH images obtained with linearly polarized radiation tuned at 776eV [Fig. 5(a)], at 777eV [Fig. 5(b), same as Fig. 4(d)] and at 778eV [Fig. 5(c)]. Total acquisition times were 24s, 140s and 400s, respectively. The images and the line profiles of Fig. 5(d) show that optimal conditions for improved transmission and contrast are found at 777eV, i.e. 1eV below the main absorption peak of the Co-L_3 edge. Figure 5 confirms in terms of FTH images, hence in a more visual way, the results of Fig. 2.

4. Discussion

Up to now, performing magnetic FTH imaging at the TM-2p and RE-3d resonances starting from a linearly polarized soft x-ray source relied on the Faraday effect in the transmission through a magnetized filter containing the element of interest [6,7]. Faraday polarizers have some drawbacks that justify the search for alternative methods:

- the polarizer reduces the intensity strongly for a moderate degree of circular polarization. For instance, estimated transmission at the SXR station of LCLS [7] is 4% at the Co 2p resonance for a polarization rate of 30%, giving an overall efficiency of the polarizer in the order of 1%;
- the polarization rate varies rapidly with the photon energy; it is maximum at the maximum of $\Delta\beta$ (hence, for Co, at the maximum of the absorption coefficient) and it diminishes quickly below the absorption maximum, where scattering experiments can take advantage of simultaneous weak absorption and strong dichroism in the real part of the optical index;
- obtaining suitable filters containing magnetically saturated ions can be difficult for certain elements, especially for light 3d-TM and for most of the RE ions, hindering the efficiency, or even the feasibility, of a transmission polarizer;
- in the case of compounds (e.g., 3d-TM oxides), the optimal energies for having, on the one hand, a high efficiency of the polarizer and, on the other hand, a strong magnetic contrast from the sample can differ due to chemical shifts, reducing the efficiency further.

Our work shows that FTH magnetic imaging with linearly polarized x-rays can be obtained by separating mask and sample and by using the sample itself as a Faraday polarizer for the reference wave. By a direct comparison of images of the same object area taken with equivalent statistics, we have shown that linear-FTH magnetic images can have the same contrast as images obtained with full circular polarization. Although quantitative estimates have to take the specific nature of the sample into account, a consistent gain in efficiency can

#163638 - $15.00 USD Received 23 Feb 2012; revised 6 Apr 2012; accepted 7 Apr 2012; published 13 Apr 2012
(C) 2012 OSA

be attained by our approach, justifying its implementation for attempting single-shot magnetic imaging experiments at 4th generation sources.

The fact of relying on the separation of mask and sample gives our approach the necessary flexibility for imaging selected areas of choice pertaining to the same sample [8]; by placing the sample before the mask, this approach may also allow one to recycle the mask in destructive single-shot experiments, which would simplify significantly the preparation since the mask is the only FIB machined part.

One usual way of increasing the magnetic contrast when using circularly polarized light is to take the difference between two images obtained with opposite helicities. Such a procedure does not apply to single-shot experiments, but it can be very important at HHG sources. Taking the difference between resonant and off-resonance images, e.g., Fig. 4(a) and Fig. 4(b), provides a rather simple way of enhancing magnetic contrast when using linearly polarized x-rays.

The possibility of imaging perpendicularly magnetized domains using linearly polarized x-rays directly was not verified experimentally to date; our work shows that this is a viable alternative to the use of circular polarization. Although our approach is unlikely to solve all experimental problems related to the polarization state of the source, it simplifies and makes more versatile the experimental set-up, offers benefits with respect to some of the drawbacks of using Faraday filters and may have a relevant impact on magnetic imaging experiments at 4th generation x-ray sources.

Acknowledgments

We thank Synchrotron SOLEIL for granting beamtime to our project. Partial financial support for this work was provided by C'Nano - Ile-de-France (TRIPEPS and DYNAVO projects) and by RTRA “Triangle de la Physique” (FibNanoSynth project). Maurizio Sacchi and Marina Tortarolo are members of the Laboratoire International Franco-Argentin en Nanosciences (LIFAN), which supported this research.

#163638 - $15.00 USD Received 23 Feb 2012; revised 6 Apr 2012; accepted 7 Apr 2012; published 13 Apr 2012
(C) 2012 OSA